Figures and tables

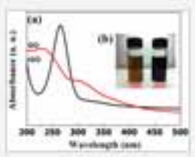

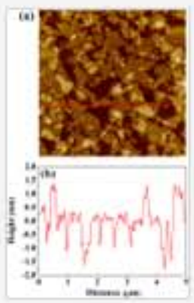

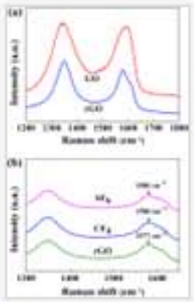

Table 1

Applied Surface Science
Volume 287, 15 December 2013, Pages 91–96

Effect of fluorine plasma treatment with chemically reduced graphene oxide thin films as hole transport layer in organic solar cells

Youn-Yeol Yu, Byung Hyun Kang, Yang Doo Lee, Sang Bin Lee, Byeong-Kwon Ju

Show more

http://dx.doi.org/10.1016/j.apsusc.2013.09.078

Get rights and content

Highlights

- The performance of organic solar cells is improved by fluorine plasma treatments on reduced graphene oxide films.
- The work function of graphene oxide film after plasma treatments increases because they consist of covalent bonds with fluorine on the surface of film.
- The device fabricated with fluorine doped graphene oxide by SF6 plasma showed the highest FF and PCE of OPVs.

Abstract

The inorganic materials such as V_2O_5, MoO_3 and WO_3 were investigated to replace PEDOT:PSS as hole transport layer (HTL) in organic electronic devices such as organic solar cells (OSCs) and organic lighting emission diodes. However, these methods require vacuum techniques that are long time process and complex. Here, we report about plasma treatment with SF_6 and CF_4 using reactive ion etching on reduced graphene oxide (rGO) thin films that are obtained using an eco-friendly method with vitamin C. The plasma treated rGO thin films have dipoles since they consist of covalent bonds with fluorine on the surface of rGO. This means it is possible to increase the electrostatic potential energy than bare rGO. Increased potential

Applied Surface Science 287 (2013) 91–96

Contents lists available at ScienceDirect

Applied Surface Science

journal homepage: www.elsevier.com/locate/apsusc

Effect of fluorine plasma treatment with chemically reduced graphene oxide thin films as hole transport layer in organic solar cells

Youn-Yeol Yu, Byung Hyun Kang, Yang Doo Lee, Sang Bin Lee, Byeong-Kwon Ju*

Display and Nanosystem Lab, College of Engineering, Korea University, Anam-dong, Seongbuk-gu, Seoul 136-713, Republic of Korea

ARTICLE INFO

Article history:
Received 5 August 2013
Received in revised form
10 September 2013
Accepted 11 September 2013
Available online 25 September 2013

Keywords:
Graphene oxide
Hole transport layer
Organic solar cells
Plasma treatments
Organic electronics

ABSTRACT

The inorganic materials such as V_2O_5, MoO_3 and WO_3 were investigated to replace PEDOT:PSS as hole transport layer (HTL) in organic electronic devices such as organic solar cells (OSCs) and organic lighting emission diodes. However, these methods require vacuum techniques that are long time process and complex. Here, we report about plasma treatment with SF_6 and CF_4 using reactive ion etching on reduced graphene oxide (rGO) thin films that are obtained using an eco-friendly method with vitamin C. The plasma treated rGO thin films have dipoles since they consist of covalent bonds with fluorine on the surface of rGO. This means it is possible to increase the electrostatic potential energy than bare rGO. Increased potential energy on the surface of rGO films is worth applying organic electronic devices as HTL such as OSCs. Consequently, the power conversion efficiency of OSCs increased more than the rGO films without plasma treatment.

1. Introduction

Graphene oxides (GO) have been used as a way to obtain graphene when the solution-based chemical reduction of GO to graphene [1,2] has previously been developed. The GO was easily obtained by exfoliation of graphite oxide using ultrasonication in a bath. The chemical reduction which changes to reduced graphene oxide (rGO) from GO was conducted using vitamin C as a reducing agent. Moreover, vitamin C, having a mild reductive ability and nontoxic property, is used in nature as a reducing agent in many living organisms. The rGO have some advantages that solution based chemical rGO include low cost, bulk scale production ability, a single layer graphene can simply be obtained by sonicating at room temperature, and the rGO can be made of thin films with a solution technique using dip-coating, [3] spin-coating, [4] spray coating, [5] and Langmuir–Blodgett assembly [6] at room temperature. The rGO-based films can be used as transparent conductors, [7] ultracapacitors, [8] field emitters, [9] and gas barriers [10]. Applied graphene-based materials have also been studied for various functional parts such as additives [11] and electrode [12] in energy conversion and storage devices [13–15]. The use of functional graphene should lead to additional improvements in organic solar cells (OSCs). Recently, graphene oxide thin films were investigated for their use as a hole transport layer (HTL) in organic electronic devices such as OSCs [16–23] and organic lighting emission diodes (OLED) [24]. The power conversion efficiency (PCE) value of a conventional device with GO thin layer (2 nm thickness) as an efficient HTL was increased to 3.50% more than device without graphene (only ITO) [25]. The advantages of rGO are that it serves to minimize the detrimental effects of indium tin oxide (ITO) roughness as well as to align the work function of either Poly (3-hexylthiophene-2,5-diyl) (P3HT) in OSCs or 1,4-bis[(1-naphthylphenyl)amino)]biphenyl in OLED and ITO for more efficient collection and emission of holes as HTL. To obtain the high performance of OSCs, rGO films require a change of work function such as p-doping with gold nanoparticles [26,27]. However, this is not only expensive but is also inefficient for devices and causes an electrical short between the ITO and the active layer due to many large particles.

In this paper, we report for the first time simply treated rGO thin films with sulfur hexafluoride (SF_6) and tetrafluoromethane (CF_4) as a new type of HTL that can be readily fabricated using reactive ion etching (RIE). Its treatment has the C—F covalent bonds. Firstly, our method starts with the synthesis of rGO by vitamin C from graphite powder followed by modified Hummer's method with sodium dodecyl benzene sulfonate (SDBS) for protection from hazardous materials and the plasma is then treated on the surface of rGO. rGO thin films as HTL increase PCE more dramatically and efficiently than bare ITO. Moreover, the SF_6 and CF_4 plasma treated rGO films increase the short circuit current density (J_{SC}) and fill factor (FF), resulting in a greater PCE increase than with rGO thin films because the effect of plasma.

* Corresponding author. Tel.: +82 2 3290 3237; fax: +82 2 3290 3791.
E-mail address: bkju@korea.ac.kr (B.-K. Ju).

0169-4332/$ – see front matter © 2013 Elsevier B.V. All rights reserved.
http://dx.doi.org/10.1016/j.apsusc.2013.09.078

2. Experimental

2.1. Materials

Graphite oxide was prepared from natural graphite powder (99.9999%, −200 mesh, Alfa Aesar), Potassium peroxodisulfate, Phosphorus pentoxide, Sulfuric acid, Hydrochloric acid, hydrogen peroxide (30 wt% aqueous solution), vitamin C, and Potassium permanganate (Sigma–Aldrich) and was used an as an oxidizing agent. SDBS was purchased from TCI, while P3HT and Phenyl-C61-butyric acid methyl ester (PCBM) were purchased from Rieke metals and Nano-C, respectively.

2.2. Preparation of reduced graphene oxide

Graphite powder was preferentially oxidized using the modified Hummer method to form graphite oxide. Typically, graphite powder (1.2 g) was added to a prepared solution of concentrated H_2SO_4 (5 mL), $K_2S_2O_8$ (1 g), and P_2O_5 (1 g). The solution was kept at 80 °C for 4.5 h, and was then diluted with deionized (DI) water (200 mL). The mixture was filtered, washed, and dried to remove any residual acid. The pretreated graphite powder (2 g) was dispersed in concentrated H_2SO_4 (46 mL) in an ice bath. The mixture was kept at 0 °C with the gradual addition of $KMnO_4$ (6 g) while stirring. The mixture was reacted at 35 °C for 2 h, and was then diluted with DI water (92 mL) and reacted at 35 °C for 2 h. The mixture was diluted with DI water (280 mL), followed by the addition of H_2O_2 (30 wt%), and was left for several seconds whereby the color changed to brilliant yellow. The mixture was filtered and washed with 1:10 HCl aqueous solution and DI water and was dialyzed for two weeks. The washed solution was dried on a Petri dish in a vacuum oven at 60 °C for one day to obtain a powder form. The presence of surfactant SDBS facilitated the exfoliation of the graphite oxide to GO and a larger size of GO sheet can be obtained in the ultrasonication process. The GO was exfoliated by sonicating 1.5 mg mL^{-1} graphite oxide solution for 2 h in the presence of SDBS. The aqueous solution was reduced by vitamin C at 80 °C for one day.

2.3. Fabrication of devices

The ITO coated glass substrates were cleaned with ultrasonication, acetone, methanol, and DI water for 30 min each, sequentially, and then dried in an oven at 120 °C for 10 min. All substrates were treated with O_2 plasma for 4 m. The GO films as interfacial layers such as rGO were spin-coated onto the O_2 plasma treated ITO/glass substrate at 1000 rpm followed by annealing of the resulting film at 120 °C for 10 min. To remove impurities such as vitamin C, the products were prepared by rinsing with ethanol followed by annealing at 120 °C for 10 min. The plasma treatment was carried out using a RIE system. The chamber was evacuated to less than 5×10^{-5} Torr at fixed parameters including work pressure, gas flow rate, and RF power that were 20 mTorr, 20 sccm, and 20 W, respectively. The etch times were performed from 10 to 60 s in a SF_6 and CF_6 environment. For the active layer, P3HT and PCBM were dissolved in mono-chlorobenzend (CB, 40 mg/ml) and blended using a mixing ratio of 10:15 for 16 h. The active layer films using blended P3HT/PCBM were spin-coated at 900 rpm for 30 s, and thermal pre-annealing was then performed at 140 °C for 10 min in a glove box in an argon atmosphere. Finally, the Al cathode (100 nm) and the interlayer (LiF 0.8 nm) were thermally evaporated in a vacuum greater than 9×10^{-8} Torr.

2.4. Characterization

Atomic force microscopy (AFM) images were taken using a XE-100 operated in tapping mode with a silicon cantilever on a silicon dioxide wafer. The silicon dioxide wafer was cleaned in prepared piranha solution (a mixture of 7:3 (v/v) 98% H_2SO_4/30% H_2O_2) at 80 °C for about ten minutes then washed in methanol and ethanol. Because piranha solution reacts violently with almost any organic material, it was handled with extreme care. The UV–vis/NIR spectra were obtained using a Carry 5000 in a quartz cell (Agilent). The Raman spectroscopy measurements were conducted using a micro-Raman system (Jobin Yvon LabRAM HR 800 UV) with excitation energy of 2.41 eV (514 nm). The X-ray photoelectron spectroscopy (XPS) measurements were performed using K-alpha (thermo electron) with monochromatized Al Kα under a pressure of 5×10^{-9} Torr on the ITO substrate. The photovoltaic characteristics were measured using a Keithley 2400 source meter and simulated AM 1.5 global solar irradiation with an incident powder density of 100 mW/cm^2 using a 300 W Xe lamp (Oriel Instrument). The work function was measured by AC-2 photoelectron spectrometer in the air (Ren Keiki Co., Ltd.).

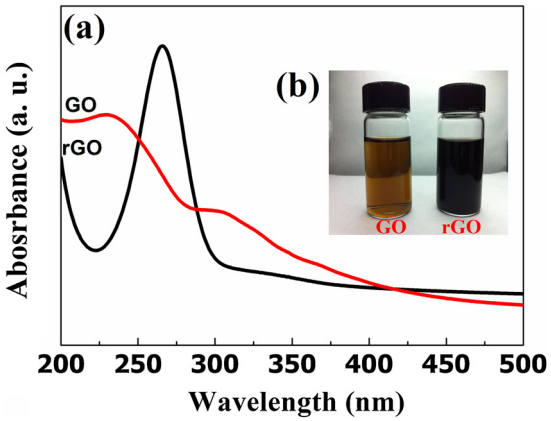

Fig. 1. UV–visible spectroscopy of GO aqueous dispersions before and after being reduced with vitamin C. Inset: optical images of GO and rGO.

3. Results and discussion

The aqueous dispersion of GO sheets was prepared using the modified Hummer's method [28]. The graphite powders were oxidized to graphite oxide using $KMnO_4/H_2SO_4$. The van der Waals forces were weak when generating GO sheets by sonication in the water because of the increased interlayer distance between the graphite oxide sheets since the graphite oxide sheets are strongly hydrophilic, such that intercalation of water molecules between the layers readily occurs. To improve the electrical conductivity of GO, we conducted a reduction of sheets from GO to rGO solutions by adding SDBS as a surfactant in the water. The reduction of GO is typically carried out using hydrazine or sodium borohydride, each of which is highly poisonous and explosive. Thus, in this study, the reduction of GO was carried out using vitamin C in the water with SDBS. The vitamin C has a mild reductive ability and nontoxic property. The results of reduction were monitored by measuring the position of the UV–visible spectra absorption peak of the aqueous rGO solution.

As shown in Fig. 1, the peak was located at 229 nm as previously reported for GO by $\pi \rightarrow \pi^*$ transitions (conjugation), but gradually red-shifts from deoxygenating occurred so that the aromatic structure was restored. A shoulder peak located at around 300 nm can be attributed to the $n \rightarrow \pi^*$ transitions of the carbonyl group [29]. Furthermore, the optical image of GO shows a transition of reduction that changed color from light brown to black aqueous suspension (see Fig. 1. inset). The AFM image shows the height profile and surface rms roughness (R_q) of the rGO sheets, which are about ~1.2 and 0.67 nm, indicating the single layer graphene [30] (see Fig. 2). This

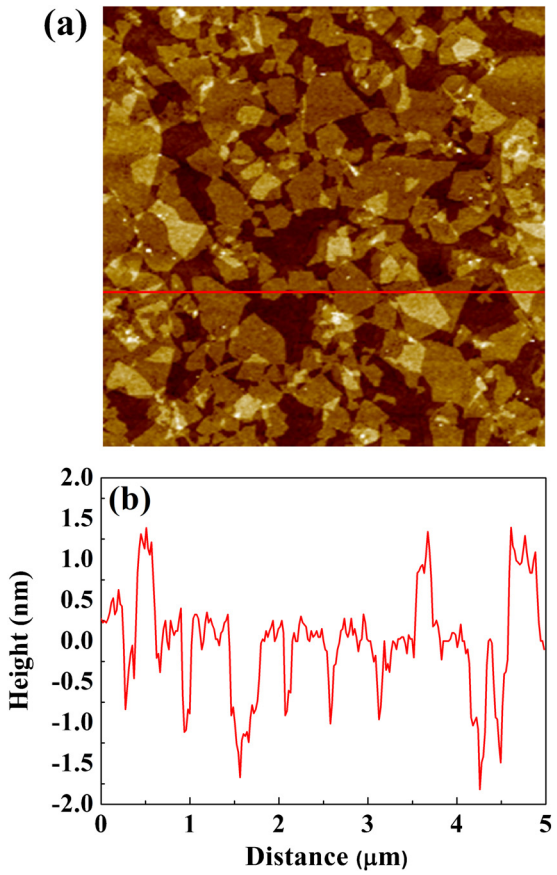

Fig. 2. (a) Tapping mode AFM topography image of rGO sheets with vitamin C onto SiO_2 substrate, and (b) the height profile of the AFM image.

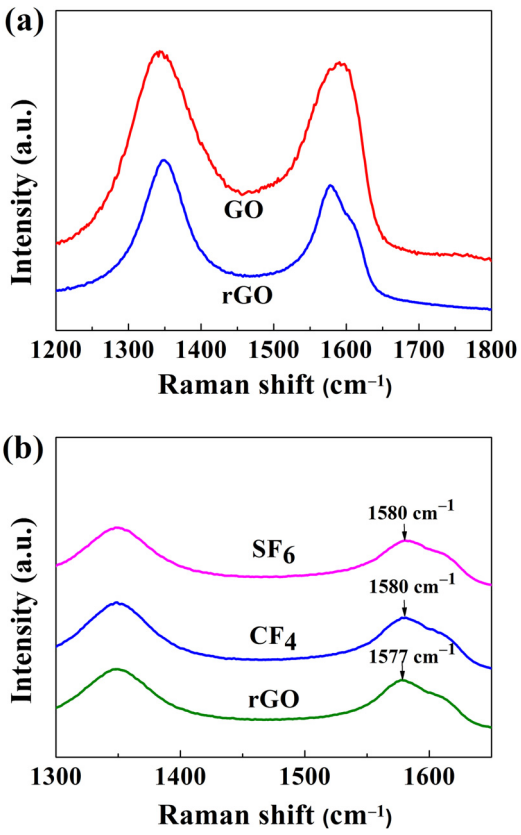

Fig. 3. (a) Raman spectra of before (red) and after, reduced with vitamin C (blue) and (b) the Raman spectra of plasma treated rGO with SF_6 and CF_4.

Table 1
Raman spectra characteristics of various plasma treated rGOs with SF_6 and CF_4.

	D Peak	G Peak	I_D/I_G
GO	1347	1590	1.03
rGO	1347	1577	1.17
SF_6 plasma treatment	1347	1580	1.20
CF_4 plasma treatment	1348	1580	1.21

is greater than the height of pure graphene due to the remaining oxygen functional groups with the surface and edge of sheets of hydroxyl, carboxyl, and carbonyl.

We conducted spin-coating on the ITO/glass substrate with GO, rGO, SF_6, and CF_4 samples for the measurements of the electronic state, defects, and functional groups of graphene characterized by Raman spectra and XPS. The Raman scattering is dependent on carbon materials and structures so that it can be characterized as a graphene material. The Raman spectra of GO and rGO vitamin C shows two main peaks at 1347 cm^{-1} (D mode), corresponding to a breathing mode of k-point photons of A_{1g} symmetry and 1590 cm^{-1} (G mode) due to the first-order scattering of the E_{2g} phonons by sp^2 carbon atoms as shown in Fig. 3a. The variation of the relative intensities of the G and D bands reveals the change of the electronic conjugation state in the Raman spectra of the GO to rGO during the reduction [31]. As shown in Table 1, the I_D/I_G ratio of rGO increased from 1.03 to 1.17 due to the restoration of the sp^2 network during the reduction process; also, the peak of rGO (1577 cm^{-1}) at the G band was down shifted compared to GO (1590 cm^{-1}), and this was attributed to the presence of isolated double bonds that resonated at frequencies lower than those of the G band of the rGO. Fig. 3b shows Raman spectra indicating defects with SF_6 and CF_4 by plasma treatments. The I_D/I_G intensity of SF_6 and CF_4 was 1.20 and 1.21, respectively, in the Raman spectra analysis, indicating that there are lowly defects and surface treatment in rGO films corresponding to the C—F bonds.

To further investigate the functional groups films were attached with GO, rGO, SF_6, and CF_4 samples characterized by XPS analysis. The C1s XPS spectra of GO before and after the reduction with vitamin C as shown in Fig. 4, showed three following peaks at 284.4, 286.4, and 287.7 eV from C=C/C—C in aromatic rings, C—O (epoxy and alkoxy), and C=O, respectively. After reduction, the intensities of all the C1s peaks of carbon binding to oxygen and sp^3 carbon gradually decreased. Especially, the C—O (epoxy and alkoxy) peak dramatically decreased, implying that most of the oxygen containing functional groups was removed after the reduction. The elemental analysis of GO indicates the presence of 59.9% carbon and 40.1% oxygen. On the other band, rGO indicates the presence of 71.39% carbon and 28.61% oxygen. Fig. 5 shows the deconvolution of the C1s and F1s spectrum of samples. As shown in Fig. 5, the C1s peaks of the functionalized GO in the CF_4 and SF_6 plasma were attributed to C—F and C—F_2 at 288.7 and 290.9 eV, respectively, indicating the covalent bonds between carbon and fluorine atoms [32]. In the same manner, the F1s peak of functionalized rGO in the CF_4 and SF_6 plasma shows the existence of two kinds of components consisting of fluorine bonding including C—F semi ionic and C—F covalent at 685.4 and 688.1 eV, respectively [33–35].

The fluorine needs to change the electrostatic potential outside the surface. The large difference in electronegativity between carbon (2.55) and fluorine (3.98) means that the C—F bonds at the surface were polar, which is equivalent to introducing a layer of dipoles across the surface. These dipoles could increase the electrostatic potential energy on the surface with covalent bonds. To apply organic electronic devices, we demonstrate here the

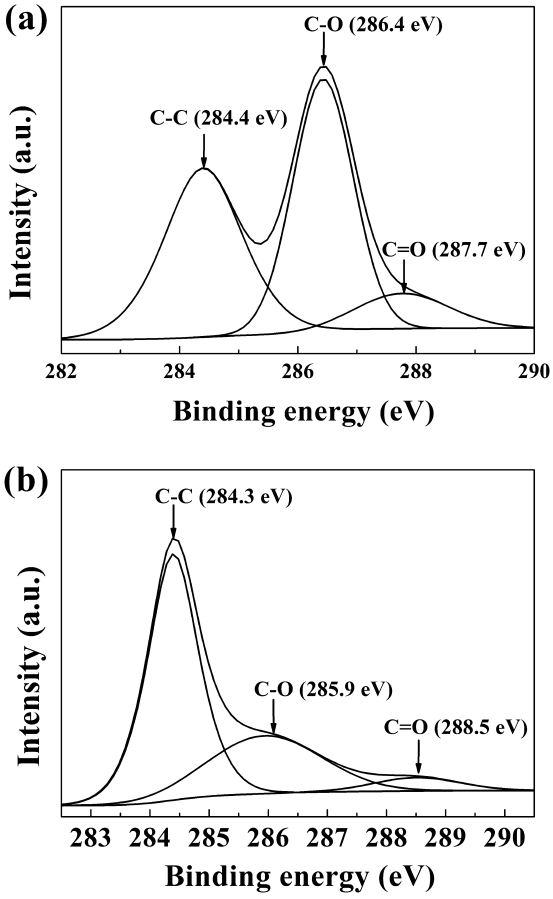

Fig. 4. The C1s XPS spectra of (a) GO and (b) rGO with vitamin C.

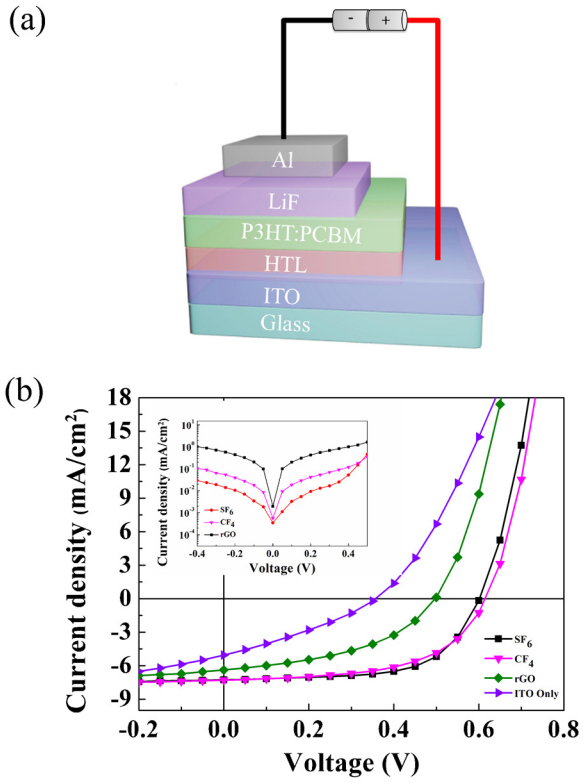

Fig. 6. (a) Device structure of OSCs, and (b) representative *J–V* curves characteristics of OSCs based on different plasma treated rGO. Inset: *J–V* dark current.

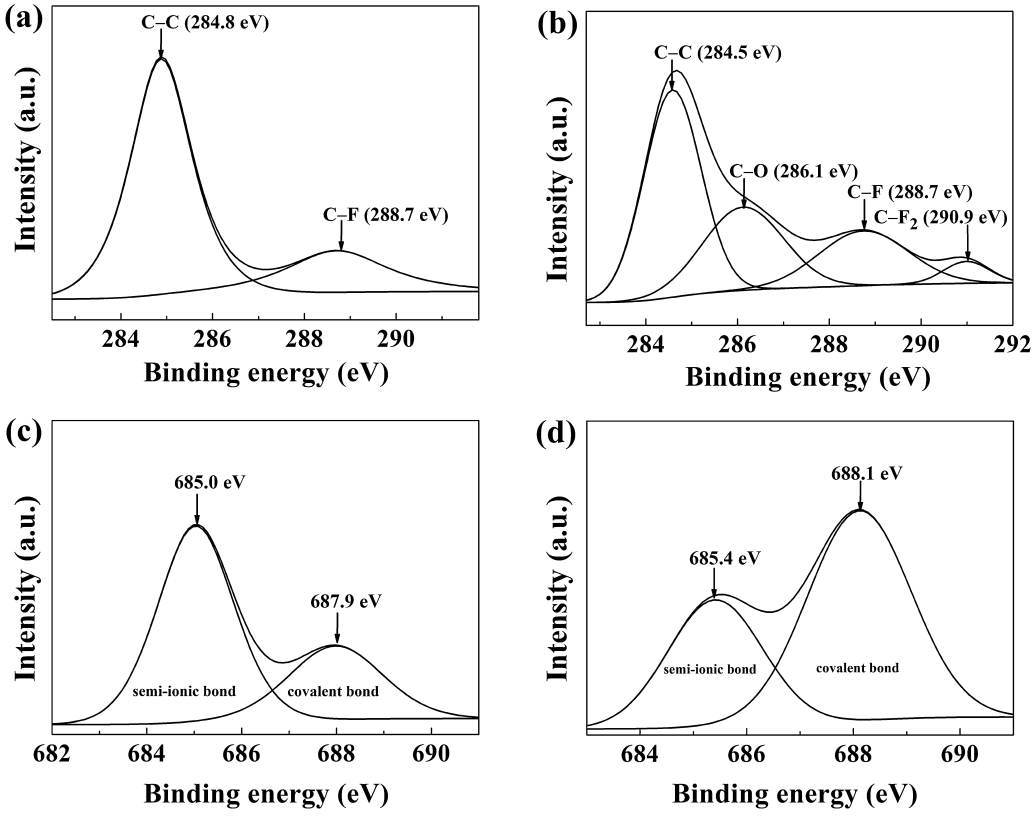

Fig. 5. The deconvoluted C1s peak of plasma treated rGO with (a) SF_6, (b) CF_4, and deconvoluted F1s peak for (c) SF_6 and (d) CF_4.

Table 2
Summary of typical photovoltaic parameters of various HTLs.

	V_{OC} (V)	J_{SC} (mA cm^{-2})	FF (%)	PCE (%)
ITO only	0.35	5.04	31.13	0.56
rGO	0.49	6.38	44.97	1.42
SF_6 plasma treatment	0.60	7.27	62.33	2.72
CF_4 plasma treatment	0.61	7.29	56.36	2.52

Table 3
Summary of PCE of rGO as per etching times in OSCs.

	PCE (%)		
	10 s	30 s	60 s
SF_6 plasma treatment	2.60	2.72	2.41
CF_4 plasma treatment	2.41	2.52	1.11

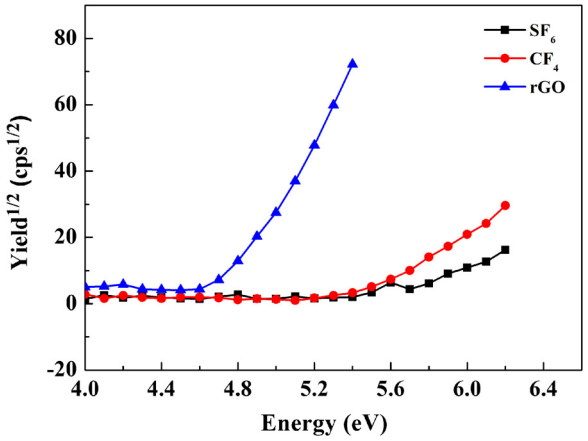

Fig. 7. Work function measurements by plasma treated rGO with SF_6, CF_4. Work function values were calculated by extrapolating two solid lines from the background and straight onset in the electron threshold region.

fabrication of OSCs device based plasma treated rGO as HTL. Fig. 6 shows the device configuration, the J/V curves and dark current of the devices. The characteristics of OSC are summarized including open circuit voltage (V_{OC}), J_{SC}, FF, and PCE as shown in Table 2. Each rGO based HTL was spin coated onto ITO/glass substrates and process plasma surface treated. It can be seen that the ITO only device shows PCE of 0.56% without HTL. The position of rGO thin film between ITO and P3HT:PCBM as a buffer layer results in a considerable increase in V_{OC}, J_{SC}, and FF, leading to an enhancement in the PCE to 1.42%. To investigate the influence of plasma etching time on the OSCs characteristics, we changed the time from 10 to 60 s, the results of which are shown in Table 3. The PCE of fluorine gas treated rGO reached a maximum at 30 s. Consequently, the cells with SF_6 and CF_4 showed V_{OC} of 0.60 and 0.61 V, J_{SC} of 7.27 and 7.29 mA cm^{-2}, FF of 62.33 and 56.36%, and PCE of 2.72 and 2.52%, respectively. These fluorine gas plasma treated rGO films increase J_{SC} and FF, resulting in a 48% and 44%, increase, respectively, in efficiency compared to plasma treatment rGO thin films. Furthermore, the dark current density with SF_6 and CF_4 plasma treated rGO films was one order lower than that of the OSCs with plasma treated rGO films (see Fig. 6. inset). Increase in efficiency of the devices is from dipole formed due to the difference in electronegativity between carbon and fluorine, which increases the work function. In order to investigate the work function by coating the GO on ITO substrate, we conducted Kelvin measurements after the fluorine plasma treatment. The rGO sample was found to be 4.7 eV, which is consistent with the previous report [36]. The work function value with CF4 and SF6 plasma treatment was found to be 5.38 and 5.48 eV (Fig. 7). The work function of SF_6 plasma treatment sample has more value than CF_4 sample because of different bond lengths. The semi-ionic/covalent ratio is 1.28 (SF_6) and 0.84 (CF_4). Longer bond lengths and higher fluorine charges were predicted for addition to graphene defect site [37].

4. Conclusions

We developed an approach for obtaining functional rGO films from plasma treatment with SF_6 and CF_4 plasma. This method is solution-processable and environmentally friendly. In particular, fluorine plasma treated rGO films create semi-ionic and covalent bonds on the surface of rGO films. Our results show that the development of simply functionalized rGO as an interfacial layer is an efficient method for organic electronic devices. Plasma treated rGO films of higher work function have a better performance in OSCs. In addition, we also studied how the plasma treated rGO films affects the HTL. Our work provides information for the wide application of graphene materials in the organic electronic devices.

Acknowledgements

This research was supported by IT convergence program of MKE/KEIT [10044003, High-performance packaging technologies and products developed for outdoor activities ensure that the service life of 25,000 h or more of Wearable Display Module], the IT R&D Infrastructure Program supervised by the NIPA (National IT Industry Promotion Agency) [NIPA-2011-(B1110-1101-0002)], and the Industrial Core Technology Development Program funded by the Ministry of Knowledge Economy (no. 10037394).

References

[1] S. Stankovich, D.A. Dikin, R.D. Piner, K.A. Kohlhaas, A. Kleinhammes, Y. Jia, Y. Jia, S.T. Nguyen, R.S. Ruoff, Synthesis of graphene-based nanosheets via chemical reduction of exfoliated graphite oxide, Carbon 45 (2007) 1558–1565.
[2] S. Park, R.S. Ruoff, Chemical methods for the production of graphenes, Nat. Nanotechnol. 4 (2009) 217–224.
[3] X. Wang, L. Zhi, K. Mullen, Transparent conductive graphene electrodes for dye-sensitized solar cells, Nano Lett. 8 (2008) 323–327.
[4] H.A. Becerril, J. Mao, Z. Liu, R.M. Stoltenberg, Z. Bao, Y. Chen, Evaluation of solution-processed reduced graphene oxide films as transparent conductors, ACS Nano 2 (2008) 463–470.
[5] V.H. Pham, T.V. Cuong, S.H. Hur, E.W. Shin, J.S. Kim, J.S. Chung, E.J. Kim, Fast and simple fabrication of a large transparent chemically converted graphene film by spray-coating, Carbon 48 (2010) 1945–1951.
[6] L.J. Cote, F. Kim, J. Huang, Langmuir–Blodgett assembly of graphite oxide single layers, J. Am. Chem. Soc. 131 (2009) 1043–1049.
[7] G. Eda, G. Fanchini, M. Chhowalla, Large-area ultrathin films of reduced graphene oxide as a transparent and flexible electronic material, Nat. Nano. 3 (2008) 270–274.
[8] M.D. Stoller, S. Park, Y. Zhu, J. An, R.S. Ruoff, Graphene-based ultracapacitors, Nano Lett. 8 (2008) 3498–3502.
[9] H.J. Jeong, H.D. Jeong, H.Y. Kim, S.H. Kim, J.S. Kim, S.Y. Jeong, J.T. Han, G.-W. Lee, Flexible field emission from thermally welded chemically doped graphene thin films, Small 8 (2012) 272–280.
[10] H. Kim, A.A. Abdala, C.W. Macosko, Graphene/polymer nanocomposites, Macromolecules 43 (2010) 6515–6530.
[11] Q. Liu, Z. Liu, X. Zhang, N. Zhang, L. Yang, S. Yin, Y. Chen, Organic photovoltaic cells based on an acceptor of soluble graphene, Appl. Phys. Lett. 92 (2008), 223303–223303–3.
[12] Z.-S. Wu, G. Zhou, L.-C. Yin, W. Ren, F. Li, H.-M. Cheng, Graphene/metal oxide composite electrode materials for energy storage, Nano Energy 1 (2012) 107–131.
[13] N.G. Sahoo, Y. Pan, L. Li, S.H. Chan, Graphene-based materials for energy conversion, Adv. Mater. 24 (2012) 4203–4210.
[14] L. Dai, Functionalization of graphene for efficient energy conversion and storage, Acc. Chem. Res. 46 (2013) 31–42.
[15] D. Chen, H. Zhang, Y. Liu, J. Li, Graphene and its derivatives for the development of solar cells photoelectrochemical, and photocatalytic applications, Energy Environ. Sci. 6 (2013) 1362–1387.
[16] J.-M. Yun, J.-S. Yeo, J. Kim, H.-G. Jeong, D.-Y. Kim, Y.-J. Noh, S.-S. Kim, B.-C. Ku, S.-I. Na, Solution-processable reduced graphene oxide as a novel alternative to PEDOT:PSS hole transport layers for highly efficient and stable polymer solar cells, Adv. Mater. 23 (2011) 4923–4928.
[17] Y.-J. Jeon, J.-M. Yun, D.-Y. Kim, S.-I. Na, S.-S. Kim, High-performance polymer solar cells with moderately reduced graphene oxide as an efficient hole transporting layer, Sol. Energy Mat. Sol. C 105 (2012) 96–102.

[18] Z. Pan, H. Gu, M.-T. Wu, Y. Li, Y. Chen, Graphene-based functional materials for organic solar cells, Opt. Mater. Exp. 2 (2012) 814–824.
[19] A. Iwan, A. Chuchmała, Perspectives of applied graphene: polymer solar cells, Prog. Polym. 37 (2012) 1805–1828.
[20] A. Chuchmała, M. Palewicz, A. Sikora, A. Iwan, Influence of graphene oxide interlayer on PCE value of polymer solar cells, Synth. Met. 169 (2013) 33–40.
[21] Q. Zheng, G. Fang, F. Cheng, H. Lei, P. Qin, C. Zhan, Low-temperature solution-processed graphene oxide derivative hole transport layer for organic solar cells, J. Phys. D: Appl. Phys. 46 (2013) 135101.
[22] H.P. Kim, A.R. bin Mohd Yusoff, J. Jang, Organic solar cells using a reduced graphene oxide anode buffer layer, Sol. Energy Mater. Sol. C 110 (2013) 87–93.
[23] A.R. bin Mohd Yusoff, H.P. Kim, J. Jang, Inverted organic solar cells with TiO_x cathode and graphene oxide anode buffer layers, Sol. Energy Mater. Sol. C 109 (2013) 63–69.
[24] Z. Zhong, Y. Dai, D. Ma, Z.Y. Wang, Facile synthesis of organo-soluble surface-grafted all-single-layer graphene oxide as hole-injecting buffer material in organic light-emitting diodes, J. Mater. Chem. 21 (2011) 6040–6045.
[25] S.-S. Li, K.-H. Tu, C.-C. Lin, C.-W. Chen, M. Chhowalla, Solution-processable graphene oxide as an efficient hole transport layer in polymer solar cells, ACS Nano 4 (2010) 3169–3174.
[26] Y. Wu, W. Jiang, Y. Ren, W. Cai, W.H. Lee, H. Li, R.D. Piner, C.W. Pope, Y. Hao, H. Ji, J. Kang, R.S. Ruoff, Tuning the doping type and level of graphene with different gold configurations, Small 8 (2012) 3129–3136.
[27] K.K. Kim, A. Reina, Y. Shi, H. Park, L.-J. Li, Y.H. Lee, J. Kong, Enhancing the conductivity of transparent graphene films via doping, Nanotechnology 21 (2010) 285205.
[28] N.I. Kovtyukhova, P.J. Ollivier, B.R. Martin, T.E. Mallouk, S.A. Chizhik, E.V. Buzaneva, A.D. Gorchinskiy, Layer-by-layer assembly of ultrathin composite films from micron-sized graphite oxide sheets and polycations, Chem. Mater. 11 (1999) 771–778.
[29] D.C. Marcano, D.V. Kosynkin, A. Sinitskii, Z. Sun, A. Slesarev, L.B. Alemany, W. Lu, J.M. Tour, Improved synthesis of graphene oxide, ACS Nano 4 (2010) 4806–4814.
[30] Y. Si, E.T. Samulski, Synthesis of water soluble graphene, Nano Lett. 8 (2008) 1679–1682.
[31] I.K. Moon, J. Lee, R.S. Ruoff, H. Lee, Reduced graphene oxide by chemical graphitization, Nat. Commun. 1 (2010) 73.
[32] H.-J. Shin, W.M. Choi, D. Choi, G.H. Han, S.-M. Yoon, H.-K. Park, S.-W. Kim, Y.W. Jin, S.Y. Lee, J.M. Kim, J.-Y. Choi, Y.H. Lee, Control of electronic structure of graphene by various dopants and their effects on a nanogenerator, J. Am. Chem. Soc. 132 (2010) 15603–21560.
[33] Y.S. Lee, T.H. Cho, B.K. Lee, J.S. Rho, K.H. An, Y.H. Lee, Surface properties of fluorinated single-walled carbon nanotubes, J. Fluorine Chem. 120 (2003) 99–104.
[34] N.O.V. Plank, R. Cheung, Functionalisation of carbon nanotubes for molecular electronics, Microelectron. Eng. 73–74 (2004) 578–582.
[35] Y.W. Zhu, F.C. Cheong, T. Yu, X.J. Xu, C.T. Lim, J.T.L. Thong, Z.X. Shen, C.K. Ong, Y.J. Liu, A.T.S. Wee, C.H. Sow, Effects of CF_4 plasma on the field emission properties of aligned multi-wall carbon nanotube films, Carbon 43 (2005) 395–400.
[36] Z. Yin, S. Wu, X. Zhou, X. Huang, Q. Zhang, F. Boey, H. Zhang, Electrochemical deposition of ZnO nanorods on transparent reduced graphene oxide electrodes for hybrid solar cells, Small 6 (2010) 307–312.
[37] C.P. Ewels, G. Van Lier, J.-C. Charlier, M.I. Heggie, P.R. Briddon, Pattern formation on carbon nanotube surfaces, Phys. Rev. Lett. 96 (2006) 216103.